



PERGAMON

Polyhedron 20 (2001) 599–606



POLYHEDRON

www.elsevier.nl/locate/poly

Reaction of $\text{Ru}(\text{PPh}_3)_3\text{Cl}_2$ with 2-(arylo)pyrimidines.
Spectral and redox characterisation of the products.
Part V. Single crystal X-ray structure of $\text{Ru}(\text{PPh}_3)_2(\text{papm})\text{Cl}_2$
(papm = 2-(phenylazo)pyrimidine)

Prasanta Kumar Santra ^a, Chittaranjan Sinha ^{a,*}, Wen-Jyh Sheen ^b, Fen-Ling Liao ^c,
Tian-Huey Lu ^b

^a Department of Chemistry, The University of Burdwan, Burdwan 713104, India

^b Department of Physics, National Tsing-Hua University, Hsinchu 300, Taiwan, ROC

^c Department of Chemistry, National Tsing-Hua University, Hsinchu 300, Taiwan, ROC

Received 23 August 2000; accepted 7 November 2000

Abstract

Reaction of 2-(arylo)pyrimidine (aapm) with $\text{Ru}(\text{PPh}_3)_3\text{Cl}_2$ in CH_2Cl_2 solution affords $[\text{Ru}(\text{PPh}_3)_2(\text{aapm})\text{Cl}_2]$ (**2**) while the reaction under refluxing conditions in EtOH isolates $[\text{Ru}(\text{PPh}_3)_2(\text{aapm})_2](\text{ClO}_4)_2 \cdot \text{H}_2\text{O}$ (**3/4**). Single crystal X-ray diffraction study of dichloro-bis(triphenylphosphine){2-(phenylazo)pyrimidine}ruthenium(II) has assigned a *cis*- $\text{Ru}(\text{PPh}_3)_2$ motif to the complex. Isomers of $[\text{Ru}(\text{PPh}_3)_2(\text{aapm})_2](\text{ClO}_4)_2$ have been characterised by ¹H NMR data and they exist in *cis-trans-cis* and *cis-cis-cis* configurations in which coordination is considered with reference to three pairs of sequence of P, P (PPh_3 abbreviated as P), N, N (N is N(pyrimidine)) and N', N' (N' is N(azo)). The complexes exhibit MLCT transitions in the visible region. Redox studies show the Ru(III)/Ru(II) couple is in the range 0.8–1.2 V vs. SCE and $[\text{Ru}(\text{PPh}_3)_2(\text{aapm})_2](\text{ClO}_4)_2$ exhibits a higher potential value than that of $[\text{Ru}(\text{PPh}_3)_2(\text{aapm})\text{Cl}_2]$. © 2001 Elsevier Science B.V. All rights reserved.

Keywords: Azopyrimidines; High potential Ru(II) complexes; Phosphine; Isomer; Structures

1. Introduction

This work stems from our interest in the exploration of chemical reactivities of arylazoheterocycles [1–9]. The chromophore is $-\text{N}=\text{N}-\text{C}=\text{N}-$. It stabilises low valent metal redox states [2,7,8]; forms oxometal complexes [10]; assists metal mediated organic transformation to incorporate atoms/groups at the *ortho*-C–H function of the pendant aryl ring [11–13]. The complexes exhibit different charge transfer transitions like MLCT (metal-to-ligand charge transfer) [2,7,8] and LLCT (ligand-to-ligand charge transfer) [3,9] and the latter is observed usually in the mixed chelate com-

plexes where one of the chelates is constituted by catecholato/dithiolato coordination.

2-(Arylo)pyrimidines (aapm) are a newly designed system and some of their coordination compounds have been reported by our group [7,8]. In the present work we wish to report two classes of mixed-ligand ruthenium(II)–arylopyrimidine complexes incorporating one and two 2-(arylo)-pyrimidine (aapm) ligands. Triphenylphosphine and Cl^- act as coligands. $\text{Ru}(\text{PPh}_3)_3\text{Cl}_2$ is used as starting complex of ruthenium. In dichloromethane, the mixing of $\text{Ru}(\text{PPh}_3)_3\text{Cl}_2$ and aapm at ambient condition gives $\text{Ru}(\text{PPh}_3)_2(\text{aapm})\text{Cl}_2$ whereas the reaction in EtOH under reflux yields $[\text{Ru}(\text{PPh}_3)_2(\text{aapm})_2]^{2+}$ as the major species. The complexes are characterised by spectroscopic studies and in one case, $\text{Ru}(\text{PPh}_3)_2(\text{aapm})\text{Cl}_2$, the structure is established by X-ray crystallography.

* Corresponding author. Tel.: +91-342-60810; fax: +91-342-64452.

E-mail address: bdnvlib@giasc101.vsnl.net.in (C. Sinha).

2. Experimental

2.1. Material

Commercial RuCl_3 was purchased from Arora Matthey, Calcutta, India and was converted into $\text{RuCl}_3 \cdot 3\text{H}_2\text{O}$ by repeated evaporation to dryness with conc. HCl . PPh_3 was obtained from E. Merck. $\text{Ru}(\text{PPh}_3)_3\text{Cl}_2$ [14] and 2-(arylozo)pyrimidines [7] were obtained as described earlier. $[\text{Bu}_4\text{N}][\text{ClO}_4]$ and MeCN for electrochemical work were purified by a reported procedure [2].

2.2. Physical measurements

Microanalyses (C, H, N) were performed using a Perkin–Elmer 2400 CHNO/S elemental analyser. Spectroscopic measurements were carried out using the following instruments: UV–Vis spectra, JASCO UV–Vis/NIR model V-570; IR spectra (KBr disk, $4000\text{--}200\text{ cm}^{-1}$), JASCO FT-IR model 420; ^1H NMR spectra, Bruker 300 MHz FT-NMR spectrometers. Molar conductances (Λ_{M}) were measured in a Systronics conductivity meter 304 model using ca. 10^{-3} M solutions in MeOH . Electrochemical measurements were carried out with the use of computer controlled EG&G PARC VersaStat model 270 electrochemical instrument using a glassy carbon disk working electrode. The solution was IR compensated and the results were collected at 298 K. The reported results are refer-

enced to the saturated calomel electrode (SCE) in acetonitrile and are uncorrected for junction potential.

2.3. Preparation of complexes dichloro-bis(triphenylphosphine){2(phenylazo)pyrimidine} ruthenium(II), $\text{Ru}(\text{PPh}_3)_2(\text{papm})\text{Cl}_2$ (**2a**)

The ligand **1a** (0.04 g, 0.23 mmol) in dry CH_2Cl_2 (10 ml) was added dropwise to a stirred solution (10 ml) of $\text{Ru}(\text{PPh}_3)_3\text{Cl}_2$ (0.2 g, 0.21 mmol) at room temperature in CH_2Cl_2 . The pink–violet solution was stirred for 1/2 h. The solution was then allowed to diffuse into hexane which was layered on the CH_2Cl_2 solution. The dark crystalline product that separated was filtered off, washed with hexane and recrystallised from dichloromethane–hexane layer, the crystals were dried in vacuo, yield 0.15 g (78%). All other ruthenium complexes were prepared by the same procedure and the yields varied from 65–75%.

2.4. bis[2-(Phenylazo)pyrimidine]-bis-(triphenylphosphine)ruthenium(II) perchlorate monohydrate, $[\text{Ru}(\text{PPh}_3)_2(\text{aapm})_2](\text{ClO}_4)_2 \cdot \text{H}_2\text{O}$ (**3/4**)

2(Phenylazo)pyrimidine was added to a suspension of $\text{Ru}(\text{PPh}_3)_3\text{Cl}_2$ (0.2 g, 0.21 mmol) in EtOH (20 ml), **1a** (0.08 g, 0.43 mmol) and the mixture was refluxed for 2 h. The resulting brown–red solution was cooled to room temperature and a saturated aqueous solution of NaClO_4 (10 ml) was added. The dark solid that precipitated was collected by filtration, washed with cold H_2O and dried in vacuo over P_4O_{10} . The dried product was dissolved in a small volume of CH_2Cl_2 and chromatographed on a silica gel column. A small greenish–blue band was eluted by $\text{C}_6\text{H}_6\text{--MeCN}$ (4:1, v/v) and the desired pink–violet band was eluted with MeCN . The solution was evaporated in air and dried over P_4O_{10} . Yield: 0.16 g, (63%). All other ruthenium complexes were prepared following similar procedures and the yields varied from 55–65%.

2.5. X-ray crystal structure and analysis

A single crystal of $\text{Ru}(\text{PPh}_3)_2(\text{papm})\text{Cl}_2$ (**2a**), suitable for X-ray diffraction, was grown by slow diffusion of hexane into dichloromethane solution at 298 K. The crystal size was $0.15 \times 0.40 \times 0.50\text{ mm}^3$. Diffraction measurements were carried out on a Siemens SMART CCD diffractometer with graphite-monochromated (Mo $\text{K}\alpha$) radiation ($\lambda = 0.71073\text{ \AA}$) at 295(2) K. The unit cell was determined and refined using setting angles of 25 reflections with 2θ angles in the range of $3\text{--}56^\circ$. A summary of the crystallographic data and structure refinement parameters are given in Table 1. Of 9420 unique reflections 3780 with $I > 2\sigma(I)$ were

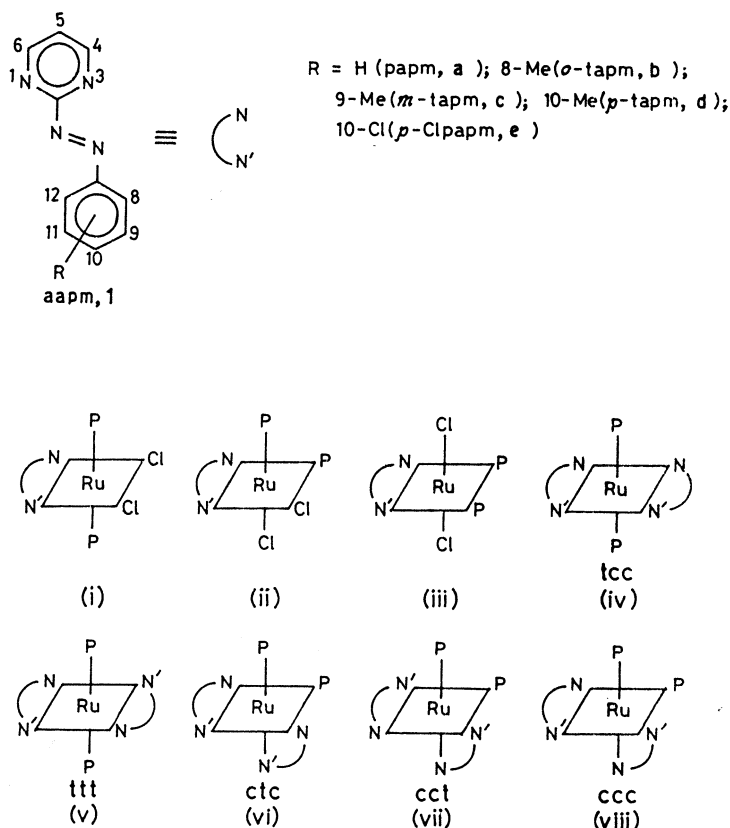
Table 1
Crystallographic data for $\text{Ru}(\text{PPh}_3)_2(\text{papm})\text{Cl}_2$ (**2a**)

Formula	$\text{C}_{46}\text{H}_{38}\text{N}_4\text{P}_2\text{Cl}_2\text{Ru}$
M	880.71
Crystal system	monoclinic
Space group	$P2_1/c$
Unit cell dimensions	
a (Å)	9.988(2)
b (Å)	17.318(4)
c (Å)	22.830(5)
β (°)	98.055(3)
V (Å ³)	3910.0(14)
λ (Å)	0.71073
ρ_{calc} (gm cm ⁻³)	1.496
Z	4
T (K)	295(2)
μ (Mo $\text{K}\alpha$) (mm ⁻¹)	0.660
Refined parameters	497
R^a [$I > 2\sigma(I)$]	0.0410
wR_2^b	0.1119
GOF ^c	0.639

$$^a R = [(F_o - F_c)/(F_o)]$$

$$^b wR_2 = [(w(F_o^2 - F_c^2))/(wF_o^4)]^{1/2}, \quad w = 1/[(2F_o^2 + (0.0712P)^2], \quad P = [\max(F_o^2, 0) + 2F_c^2]/3.$$

^c GOF is defined as $[w(F_o - F_c)/(n_o - n_v)]^{1/2}$, where n_o and n_v denote the numbers of data and variables, respectively.



Scheme 1.

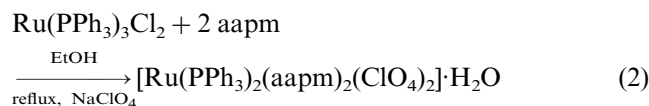
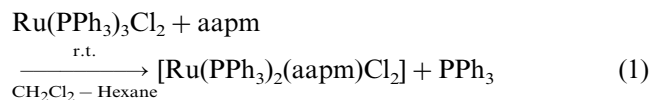
used for the structure solution. Data corrections for L_p effects and for linear-decay on ψ -scans were applied [15]. Data reductions and structure refinement were performed using SHELXS-97 [16] and successive difference Fourier synthesis. The structure was solved by the conventional heavy-atom method and refined by the full-matrix least-squares method on all F_o^2 data using the SHELXL-97 [17] package on a digital-ALFA 200 computer. All non-hydrogen atoms were refined anisotropically. The hydrogen atoms were fixed geometrically and refined using the riding model. In the final difference Fourier map the residual maxima and minima were 0.394 and $-0.464 \text{ e } \text{Å}^{-3}$.

3. Results and discussion

3.1. Synthesis

A dichloromethane solution of $\text{Ru}(\text{PPh}_3)_3\text{Cl}_2$ and 2-(arylamino)pyrimidine (aapm) in equimolar proportion on slow diffusion into hexane at ambient condition isolates a dark brown crystalline product of composition $\text{Ru}(\text{PPh}_3)_2(\text{aapm})\text{Cl}_2$ (**2**) (Eq. (1)). The reaction of $\text{Ru}(\text{PPh}_3)_3\text{Cl}_2$ and aapm in a 1:2 molar ratio in ethanol solution under reflux synthesises an ionic product which

is isolated as the perchlorate salt, $[\text{Ru}(\text{PPh}_3)_2(\text{aapm})_2](\text{ClO}_4)_2 \cdot \text{H}_2\text{O}$ (**3/4**) (Eq. (2)).



2-(Arylamino)pyrimidine (aapm, **1**) is an unsymmetrical N,N'-donor chelating ligand. $\text{Ru}(\text{PPh}_3)_2(\text{aapm})\text{Cl}_2$ may exist in *cis*- RuCl_2 (i and ii) and *trans*- RuCl_2 (iii) configurations. Only one isomer is isolated and is established structurally as *cis*-configuration. The structure of $\text{Ru}(\text{PPh}_3)_2(\text{papm})\text{Cl}_2$ (**2a**) has been confirmed by single crystal X-ray structure.

Pseudo-octahedral $[\text{Ru}(\text{PPh}_3)_2(\text{aapm})_2]^{2+}$ may exist in five geometrical isomeric forms (iv–viii) with consideration to the coordination pair sequence P, P (PPh_3 is abbreviated as P), N, N ($\text{N}(\text{pym})$ refers to N), N', N' ($\text{N}(\text{azo})$ refers to N'). The isomers are *trans*-*cis*-*cis* (*tcc*), *trans*-*trans*-*trans* (*ttt*), *cis*-*trans*-*cis* (*ctc*), *cis*-*cis*-*trans* (*cct*) and *cis*-*cis*-*cis* (*ccc*) (Scheme 1). The isomers have not been separated by chromatographic

separation. ^1H NMR spectral studies have been useful to identify the isomers that are formed; two isomers are characterised, namely *cis*- and *ccc*- $[\text{Ru}(\text{PPh}_3)_2(\text{aapm})_2](\text{ClO}_4)_2 \cdot \text{H}_2\text{O}$.

3.2. Molecular structure

The crystal structure of $\text{Ru}(\text{PPh}_3)_2(\text{papm})\text{Cl}_2$ (**2a**) is shown in Fig. 1. The bond parameters are listed in Table 2. The coordination around ruthenium is approximately octahedral. The atomic arrangement involves sequentially *trans*-phosphine, *cis*-chlorine and azoimine chelate within the $\text{RuP}_2\text{N}_2\text{Cl}_2$ coordination sphere. The atomic group $\text{Ru}, \text{Cl}(1), \text{Cl}(2), \text{N}(1), \text{N}(2)$ constitute a good plane (mean deviation < 0.06 Å). 2-(Phenyl-azo)pyrimidine is chelated with Ru and the atomic group $\text{Ru}, \text{N}(1), \text{N}(4), \text{C}(41), \text{N}(2)$ in the chelate ring con-

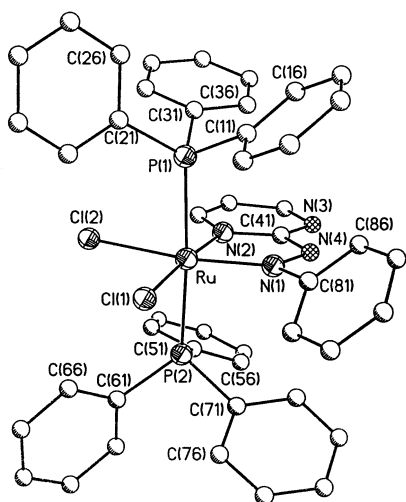


Fig. 1. Single crystal X-ray structure and the atom-labelling scheme for $\text{Ru}(\text{PPh}_3)_2(\text{papm})\text{Cl}_2$ (**2a**). For clarity, all hydrogen atoms have been omitted.

Table 2
Selected bond lengths (Å) and bond angles ($^\circ$) for $\text{Ru}(\text{PPh}_3)_2(\text{papm})\text{Cl}_2$ (**2a**) with their estimated standard deviation in parentheses

Bond lengths			
Ru–P(1)	2.4244(13)	Ru–N(1)	1.968(3)
Ru–P(2)	2.4303(13)	Ru–N(2)	2.015(3)
Ru–Cl(1)	2.4276(13)	N(1)–N(4)	1.309(4)
Ru–Cl(2)	2.4283(13)	C(41)–N(2)	1.361(5)
Bond angles			
P(1)–Ru–Cl(1)	90.98(4)	P(2)–Ru–N(1)	93.22(10)
P(1)–Ru–Cl(2)	85.79(4)	P(2)–Ru–N(2)	87.71(10)
P(2)–Ru–Cl(1)	90.59(4)	N(1)–Ru–N(2)	77.14(15)
P(2)–Ru–Cl(2)	89.89(4)	Cl(1)–Ru–Cl(2)	90.22(4)
P(1)–Ru–N(1)	90.77(10)	P(1)–Ru–P(2)	175.42(4)
P(1)–Ru–N(2)	90.99(10)	N(2)–Ru–Cl(1)	176.06(11)
N(1)–Ru–Cl(1)	99.42(11)	N(2)–Ru–Cl(2)	93.33(11)
N(1)–Ru–Cl(2)	169.82(11)		

stitutes an excellent plane (mean deviation ~ 0.01 Å). The pendant phenyl ring (C(81)–C(86)) is inclined at an acute angle ($\sim 44.6^\circ$) with the chelate ring. Two PPh_3 are *trans* and P(1)–Ru–P(2) angle is $175.42(4)^\circ$ and is in agreement with the reported results [18]. The chelate bite angle N(1)–Ru–N(2) is $77.14(15)^\circ$. The *trans*–*cis*– $\text{RuP}_2\text{N}_2\text{Cl}_2$ coordination sphere shows large deviations from octahedral geometry and it is assumed that much of it originates from the acute bite angle of the azoimine chelate.

The Ru–N(1) (N(azo)) bond distance is shorter than the Ru–N(2) (N(pyrimidine)) bond distance by 0.05 Å. The shortening may be due to π -back bonding in $d(\text{Ru}) \rightarrow \pi^*(\text{azo})$. The N–N distance is 1.309(4) Å and is comparable with reported results of $\text{Ru}(\text{papm})_2\text{Cl}_2$ [8]. The N–N bond distance for the free ligand is not available, however, the data available in some free azo ligands suggest that is ca. 1.25 Å [19]. In the present example the N–N distance is elongated by ca. 0.06 Å. This may be due to strong π -back bonding $d(\text{Ru}) \rightarrow \pi^*(\text{azo})$ (supported by spectral data). The Ru–P and Ru–Cl distances are comparable with reported results [20,21].

3.3. Spectra

IR spectra of $\text{Ru}(\text{PPh}_3)_2(\text{aapm})\text{Cl}_2$ (**2**) exhibit two sharp stretches at 350 and 300 cm^{-1} which correspond to $\nu(\text{Ru}–\text{Cl})$ and indicate a *cis*- RuCl_2 configuration. A sharp stretch at $1380\text{--}1390\text{ cm}^{-1}$ corresponds to $\nu(\text{N}=\text{N})$ and this is red shifted by $40\text{--}50\text{ cm}^{-1}$ compared to the free ligand value ($\sim 1430\text{ cm}^{-1}$) [8]. The complexes (**3/4**) exhibit a broad band centred at 3445 cm^{-1} , corresponding to $\nu(\text{H}_2\text{O})$ and this band was eliminated on cautious slow heating (perchlorates are explosive) in the $90\text{--}100^\circ\text{C}$ range [6]. Sharp stretches at $1395\text{--}1400$ and $1575\text{--}1580\text{ cm}^{-1}$ in these complexes (**3/4**) are assigned to $((\text{N}=\text{N}))$ and $((\text{C}=\text{N}))$, respectively. The bands are at relatively high energy positions in **3/4** compared to $\text{Ru}(\text{PPh}_3)_2(\text{aapm})\text{Cl}_2$ (**2**). This may be due to the competition between two π -acidic azoimine groups in $[\text{Ru}(\text{PPh}_3)_2(\text{aapm})_2]^{2+}$ compared to one azoimine group in $\text{Ru}(\text{PPh}_3)_2(\text{aapm})\text{Cl}_2$. Besides, *trans* orientation of two chelated azoimine groups in (iv)/(v) will give rise to competition for the same metal d-orbital and may not perturb N=N stretching frequency significantly. In $[\text{Ru}(\text{PPh}_3)_2(\text{aapm})_2]^{2+}$ $\nu(\text{N}=\text{N})$ is red shifted by $30\text{--}40\text{ cm}^{-1}$ compared to free ligand value ($\sim 1430\text{ cm}^{-1}$) [8]. This suggests that there may be *cis*-orientation, (vi)–(viii), in the complexes. The perchlorate vibration of the complexes is seen at 1100 cm^{-1} together with weak band at $615(625\text{ cm}^{-1})$ [22].

The solution electronic spectra of the complexes were recorded in CH_2Cl_2 for $\text{Ru}(\text{PPh}_3)_2(\text{aapm})\text{Cl}_2$ (**2**) and in MeCN for $[\text{Ru}(\text{PPh}_3)_2(\text{aapm})_2](\text{ClO}_4)_2 \cdot \text{H}_2\text{O}$ (**3/4**) in the $200\text{--}900\text{ nm}$ range. Transitions below 400 nm are

Table 3
Microanalytical ^a, UV–Vis spectral ^b and voltammetric data ^c

Compound	Elemental analyses (%)			UV–Vis spectral data ($\lambda_{\text{max}}/\text{nm}$) ($10^{-3}\epsilon \text{ M}^{-1} \text{ cm}^{-1}$)	CV data E° (V) (ΔE_p , mV)	
	C	H	N		Ru(III)/Ru(II)	Ligand reduction
Ru(P) ₂ (papm)Cl ₂ (2a)	62.64 (62.73)	4.24 (4.32)	6.28 (6.36)	770 ^d (0.17), 532(4.20), 378(11.00), 360 ^d (10.72), 285(21.01)	0.897(70)	–0.824(120), –1.147 ^c
Ru(P) ₂ (<i>o</i> -tapm)Cl ₂ (2b)	63.00 (63.08)	4.38 (4.47)	6.18 (6.26)	852 ^d (0.18), 520(3.57), 374(6.64), 342 ^d (5.54), 284(21.28)	0.875(80)	–0.847(100), –1.118 ^c
Ru(P) ₂ (<i>m</i> -tapm)Cl ₂ (2c)	63.18 (63.08)	4.55 (4.47)	6.34 (6.26)	750 ^d (0.11), 532(2.79), 382(8.20), 350(8.13), 282 ^d (1.62)	0.873(80)	–0.845(120), –1.120 ^c
Ru(P) ₂ (<i>p</i> -tapm)Cl ₂ (2d)	63.20 (63.08)	4.55 (4.47)	6.35 (6.26)	775 ^d (0.19), 530(4.32), 585(11.24), 358 ^d (10.54), 286(21.32)	0.870(80)	–0.848(110), –1.118 ^c
Ru(P) ₂ (<i>p</i> -Clpapm)Cl ₂ (2e)	60.26 (60.36)	6.22 (6.12)	4.15 (4.05)	768 ^d (0.10), 521 (2.65), 375(6.43), 345 ^d (5.47), 280(18.74)	0.922(90)	–0.801(110), –1.044 ^c
[Ru(P) ₂ (papm) ₂](ClO ₄) ₂ · H ₂ O (3a/4a)	55.45 (55.54)	3.87 (3.97)	9.35 (9.26)	894 ^d (0.24), 750(0.42), 520(3.41), 378(8.25), 348 ^d (8.99), 262(18.54)	1.21(100) 1.084(90)	–0.93(110), –1.15(100)
[Ru(P) ₂ (<i>o</i> -tapm) ₂](ClO ₄) ₂ · H ₂ O (3b/4b)	57.32 (56.22)	4.29 (4.20)	9.15 (9.05)	892 ^d (0.13), 744(0.31), 530(3.35), 370(6.02), 344 ^d (5.61), 260(15.31)	1.13(130) 0.973(100)	–1.00(120), –1.28(140)
[Ru(P) ₂ (<i>m</i> -tapm) ₂](ClO ₄) ₂ · H ₂ O (3c/4c)	56.33 (56.22)	4.11 (4.20)	9.14 (9.05)	890 ^d (0.14), 742(0.64), 522(6.72), 378(14.09), 350 ^d (15.10), 262(14.11)	1.11(110) 0.958(80)	–1.01(110), –1.30(140)
[Ru(P) ₂ (<i>p</i> -tapm) ₂](ClO ₄) ₂ · H ₂ O (3d/4d)	56.10 (56.22)	4.10 (4.20)	8.95 (9.05)	896 ^d (0.25), 745(0.47), 530(3.51), 370(10.64), 345 ^d (11.24), 264(18.65)	1.13(100) 0.960(90)	–1.00(100), –1.30(130)
[Ru(P) ₂ (<i>p</i> -Clpapm) ₂]- (ClO ₄) ₂ ·H ₂ O (3e/4e)	52.45 (52.54)	3.50 (3.60)	8.85 (8.76)	889 ^d (0.12), 742(0.35), 520(2.98), 372(8.07), 342 ^d (8.64), 260(17.31)	1.27(100) 1.118(100)	–0.88(110), –1.10(100)

^a Calculated values are in parentheses.

^b Solvent: CH₂Cl₂, for Ru(P)₂(aapm)Cl₂; CH₃CN, for [Ru(P)₂(aapm)₂](ClO₄)₂·H₂O.

^c Solvent in CH₃CN, supporting electrolyte, TBAP (0.01 M); solute concentration, 10^{–3} M; scan rate, 0.05 V s^{–1}.

^d Shoulder.

^e Cathodic peak potential, E_{pc} (V).

assigned to intra-ligand charge transfer ($n \rightarrow \pi^*$ and $\pi \rightarrow \pi^*$) and are not considered further. The spectral data are summarised in Table 3. The complexes **2** exhibit two consecutive transitions, one high intense band ($\epsilon \sim 10^4$) at 520–530 nm and a shoulder at longer wave length, 750–850 nm. [Ru(PPh₃)₂(aapm)₂]²⁺ show three transitions in the visible region: one high intense transition ($\epsilon \sim 10^4$) at 520–530 nm and two shoulders at 740–750 and 885–895 nm. Diamagnetic octahedral d⁶ transition metal complexes in principle, exhibit mainly ¹A_{1g} → ¹T_{1g} and ¹A_{1g} → ¹T_{2g} transitions in the visible region. The high intensity band does not conform to the simple d–d transition. Ruthenium(II) complexes of π -acidic azoimine systems exhibit metal-to-ligand charge transfer transitions [23]. Thus, we conclude that high intensity ($\epsilon \sim 10^4$) bands are due to a spin allowed

singlet–singlet transition and the low energy shoulders refer to ¹A_{1g} → ¹T_{1g}, ¹A_{1g} → ¹T_{2g} transitions. Assignment of the spectral transition to the stereochemistry of the complex is very difficult.

The ¹H NMR spectra of the complexes were obtained in CDCl₃ and have well defined aromatic and aliphatic regions. The proton numbering pattern is shown in Scheme 1. The spectral data are collected in Table 4. The aromatic zone of the spectra is very complex due to the phenyl protons in PPh₃. The NMR spectra of the ligands and their ruthenium(II) complexes reported elsewhere [7,8] are helpful in assigning the resonance of protons in present series of the complexes. The proton-numbering pattern is shown in aapm (**1**) and assignments are made on the basis of spin–spin interactions and changes therein upon substi-

Table 4
¹H NMR data for the complexes ^a

Compound	δ /ppm (J/Hz)								
	4-Hd	5-Ht	6-Hd	8-H	12-Hd	9-H	11-H	10-H	R
(2a)	8.65 (6.0)	7.53 (7.4)	8.29 (6.0)	7.14d (8.0)	7.14 (8.0)	6.81t (8.0)	6.81t (8.0)	6.42 (8.0)	
(2b)	8.63 (6.2)	7.50 (7.4)	8.26 (6.0)		7.12 (8.0)	6.64d (8.0)	6.78t (8.0)	6.45t (8.0)	2.68
(2c)	8.62 (6.2)	7.50 (7.4)	8.27 (6.0)	6.82s	7.10 (8.0)		6.74t (8.0)	6.40d (8.0)	2.55
(2d)	8.63 (6.0)	7.51 (7.4)	8.26 (6.2)	7.10d (8.0)	7.10 (8.0)	6.54d (8.0)	6.54d (8.0)		2.48
(2e)	8.68 (6.0)	7.56 (7.0)	8.31 (6.0)	7.27d (8.0)	7.27 (7.4)	6.89d (8.0)	6.89d (8.0)		
(3a/4a)	8.68 (6.0)	7.89 (7.4)	8.19 (6.2)	7.20d	7.13 (7.4)	6.92t (8.0)	6.92t (8.0)	6.83m	
(3b/4b)	8.66 (6.2)	7.88 (7.4)	8.14 (6.2)		7.10 (8.0)	6.60d (8.0)	6.72t (8.0)	6.70m	2.65, 250, 2.32
(3c/4c)	8.66 (6.2)	7.86 (7.0)	8.14 (6.0)	6.75s	7.05 (8.0)		6.79t (8.0)	6.60d (8.0)	2.50, 2.36, 2.17
(3d/4d)	8.65 (6.0)	7.85 (7.0)	8.15 (6.0)	7.14d (8.0)	7.00 (8.0)	6.66d (8.0)	6.88d (8.0)		2.50, 2.44, 2.35
(3e/4e)	8.86 (6.0)	7.90 (7.0)	8.20 (6.0)	7.27d (8.0)	7.18 (8.0)	7.18d (8.0)	6.91d (8.0)		

^a Solvent CDCl₃ at 295(2) K. Ph protons of PPh₃ appear at 7.1–7.2 and 7.4–7.6 ppm. d, doublet; t, triplet; s, singlet; m, multiplet.

tution. PPh₃ protons appear as broad high intense signals at 7.2–7.3 and 7.5–7.6 ppm.

The signals in the aromatic region are due to protons from aapm and PPh₃. Pyrimidine protons (4-H–6-H) appear on the downfield side (7.5–8.7 ppm) while aryl protons (8-H–12-H) exhibit resonance on the upfield side. The latter signals are affected by substitution: 9- and 11-H are perturbed due to change in the electronic properties of the substituent in the tenth position [24,25]. The –Me substituent (in *p*-tapm) moves the signal upfield due to a +I effect and the 10-Cl substituent (in *p*-Clpapm) moves them downfield because of the electron withdrawing effect of the group. The 9-Me substituent (in *m*-tapm) results in a singlet resonance that corresponds to 8-H. In *o*-tapm, the 9-H signal is heavily perturbed in comparison with the 9-H signal in *p*-tapm.

The resonance in the aliphatic region is diagnostic and has been used to assign the number and population of isomers in the mixture. There are three Ar–Me signals in [Ru(PPh₃)₂(tapm)₂]²⁺ and of these two are of equal intensities (Fig. 2). Five geometrical isomers are possible in this series of complex, (iv)–(viii), and three of these have *cis*-Ru(PPh₃)₂ configuration: *ctc*, *cct* and *ccc*. In the series of Ru(aapm)₂Cl₂ complexes two isomers had been characterised with *cis*-RuCl₂ configuration. This provides us with a guide to identify isomers in the present series. Additionally, [Ru(PPh₃)₂-(RaaIX)]²⁺ (RaaIX = 1-(alkyl-2-(arylo)imidazole)) exists as two isomers and the aliphatic region of the ¹H NMR spectra is comparable with the present examples. Thus, we may assume that two isomers *ctc*- and *ccc*-[Ru(PPh₃)₂(tapm)₂]²⁺ exist in the mixture. The *ctc* configuration has C₂-symmetry and should exhibit single a Ar–Me signal while the *ccc*-configuration belongs

to C₁-symmetry and is expected to exhibit two –Me signals of equal intensities. This is indeed observed (Fig. 2). The ratio of signal intensities is approximately 0.4:1 with respect to *ctc*-: *ccc*- configuration. Thus, the *ccc*-isomer predominates in the mixture. The higher δ in *ccc*-geometry may be due to better stabilisation in the C₁-geometry and needs an extensive stereochemical rearrangement during complexation. Pyrimidine (4-H–6-H) and aryl protons (8-H–12-H) (3/4) are assigned by comparing with the spectra of Ru(PPh₃)₂(aapm)Cl₂ (Fig. 3). Usually pyrimidine protons appear at the downfield side and aryl protons, affected by the substituent, are at an upfield position.

Being a bulky group, PPh₃ has an inherent disadvantage in stabilizing the *cis*-configuration in *cis*-Ru(PPh₃)₂ due to steric crowding. However, there are two competing forces: steric crowding between PPh₃⋯PPh₃ and π -back bonding between t₂(Ru) and π (PPh₃/aapm). The latter effect predominates in the *cis*-configuration. There are two metal d π -orbitals are available for π -ac-

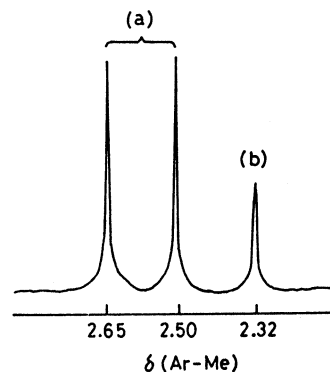


Fig. 2. Ar–Me Signals of [Ru(P)₂(*o*-tapm)₂]²⁺ denoting (a) *ccc*- and (b) *ctc*-isomers in 1:0.4 ratio, respectively.

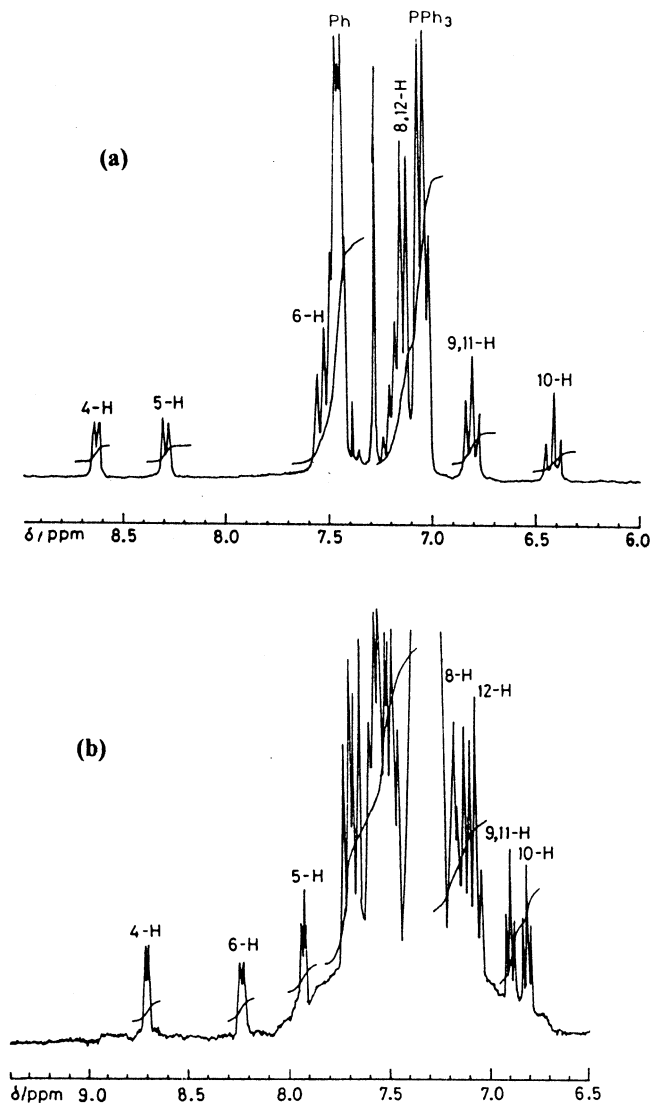


Fig. 3. ^1H NMR spectra of (a) $\text{Ru}(\text{P})_2(\text{papm})\text{Cl}_2$ and (b) $[\text{Ru}(\text{P})_2(\text{papm})_2]^{2+}$ in CDCl_3 .

ceptance in the *cis*-geometry compared to one $d\pi$ -orbital in the *trans*-geometry [26,27].

3.4. Electrochemistry

The electrochemical behaviour of the complexes was examined in MeCN under N_2 atmosphere cyclic voltammetrically using a glassy carbon working electrode with Bu_4NClO_4 as the supporting electrolyte. The voltammogram displays metal oxidation at the positive side and ligand reductions at the negative side with respect to SCE. The results are given in Table 3 and a representative voltammogram is shown in Fig. 4.

In the potential range $+0.5$ – 1.5 V at a scan rate 50 mV s^{-1} a reversible to quasi-reversible (peak-to-peak separation, $\Delta E_p = 70$ – 90 mV) oxidative response at 0.8 – 0.9 V versus SCE corresponding to the couple (1) is observed for $\text{Ru}(\text{PPh}_3)_2(\text{aapm})\text{Cl}_2$.

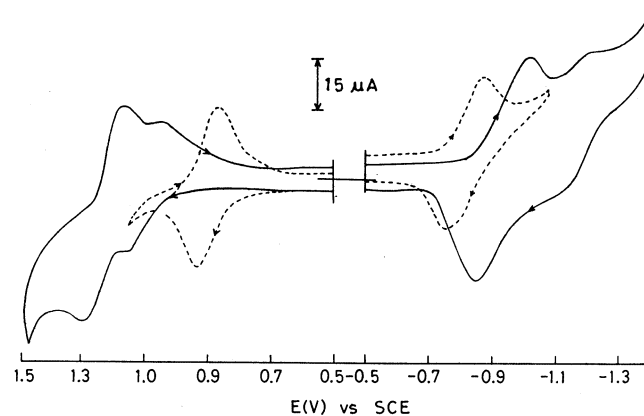
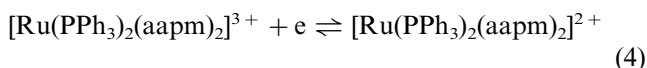
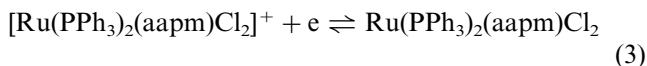


Fig. 4. Cyclic voltammogram in MeCN (0.1 M Bu_4NClO_4) at a GC-working electrode. The solute concentration and scan rate are 10^{-3} M and 50 mV s^{-1} , respectively for $\text{Ru}(\text{P})_2(\text{papm})\text{Cl}_2$ (---) and $[\text{Ru}(\text{P})_2(\text{papm})_2](\text{ClO}_4)_2$ (—).



An identical experiment for $[\text{Ru}(\text{PPh}_3)_2(\text{aapm})_2](\text{ClO}_4)_2$ exhibits two consecutive redox responses in the potential range 0.90–1.00 and 1.1–1.2 V versus SCE. They correspond to electron transfer as in couple (4). The two responses may be ascribed to different isomers present in the mixture. $[\text{Ru}(\text{PPh}_3)_2(\text{aapm})_2]^{2+}$ exist in two isomeric forms (vide supra). Thus, the Ru(III)/Ru(II) couple at 0.9–1.0 may refer to the redox response for *ctc*- $[\text{Ru}(\text{PPh}_3)_2(\text{aapm})_2](\text{ClO}_4)_2$ and that at 1.0–1.2 V for *ccc*- $[\text{Ru}(\text{PPh}_3)_2(\text{aapm})_2](\text{ClO}_4)_2$. The *ccc*-isomer shows a higher Ru(III)/Ru(II) couple than that of the *ctc*-isomer. This may be due to reduced symmetry (C_1 -symmetry) in the *ccc*-isomer relative to the *ctc*-(C_2 -symmetry) isomer; which may lead to better Ru–L interaction. Besides, the couple height is very informative in accounting the isomeric ratio in the mixture. It varies for different complexes and lies in the range 0.3:1–0.45:1. The ratio refers to the ratio of the couple of the height of the *ctc*-isomer to the *ccc*-isomer. This also supports the presence of *ccc*- $[\text{Ru}(\text{PPh}_3)_2(\text{aapm})_2](\text{ClO}_4)_2$ in higher amounts in the mixture (vide supra).

The data (Table 3) reveal that the Ru(III)/Ru(II) potential is lowered by 0.1–0.3 V on going from $[\text{Ru}(\text{PPh}_3)_2(\text{aapm})_2]^{2+}$ to $\text{Ru}(\text{PPh}_3)_2(\text{aapm})\text{Cl}_2$. This is certainly due to the replacement of π -acidic aapm by 2Cl^- groups from (3/4) to give (2). The increased π -acidity around Ru(II) enhances the M–L π -back bonding and thus $t_2(\text{Ru})$ is stabilised. The reductive responses are observed in the potential range –0.5 to –1.8 V versus SCE. The reduced species appears to be less stable and on scan reversal multiple anodic responses are observed and are assumed to be due to the reduction of the azo function. The reductive responses are compared with the results for free ligands [7]. There are two/three responses are observed and the first response is quasi-reversible ($\Delta E_p = 80$ –120 mV) whereas other responses are irreversible with a high negative E_{pc} value.

4. Supplementary material

Crystallographic data for the structural analysis have been deposited with the Cambridge Crystallographic Data Centre, CCDC no. 148063. Copies of this information may be obtained from The Director, CCDC, 12 Union Road, Cambridge, CB2 1EZ, UK (fax: +44-

1233-336033; e-mail: deposit@ccdc.cam.ac.uk or www: http://www.ccdc.cam.ac.uk).

Acknowledgements

Financial assistance from the University Grants Commission, New Delhi, India is gratefully acknowledged. Our sincere thanks are also due to Dr S. Chattopadhyay, Vidyasagar University, Midnapore for helpful discussion.

References

- [1] T.K. Misra, D. Das, C. Sinha, Polyhedron 16 (1997) 4163.
- [2] T.K. Misra, D. Das, C. Sinha, P. Ghosh, C.K. Pal, Inorg. Chem. 37 (1998) 1672.
- [3] D. Das, C. Sinha, Transition Met. Chem. 23 (1998) 517.
- [4] D. Das, A.K. Das, C. Sinha, Talanta 48 (1999) 1031.
- [5] T.K. Misra, C. Sinha, Indian J. Chem. 38A (1999) 346.
- [6] S. Pal, T.K. Misra, C. Sinha, Transition Met. Chem. 25 (2000) 333.
- [7] P.K. Santra, D. Das, T.K. Misra, R. Roy, C. Sinha, S.-M. Peng, Polyhedron 18 (1999) 1909.
- [8] P.K. Santra, T.K. Misra, D. Das, C. Sinha, A.M.Z. Slawin, J.D. Woollins, Polyhedron 18 (1999) 2869.
- [9] R. Roy, P. Chattopadhyay, C. Sinha, S. Chattopadhyay, Polyhedron 15 (1996) 336.
- [10] S. Goswami, A.R. Chakravarty, A. Chakravorty, J. Chem. Soc., Chem. Commun. (1982) 1288.
- [11] C.K. Pal, S. Chattopadhyay, C. Sinha, D. Bandyopadhyay, A. Chakravorty, Polyhedron 13 (1994) 999.
- [12] B.K. Santra, P. Munsu, G. Das, P. Bharadwaj, G.K. Lahiri, Polyhedron 18 (1999) 617.
- [13] A. Saha, A.K. Ghosh, P. Majumder, K.N. Mitra, S. Rajak, L.R. Falvello, S. Goswami, Organometallics 18 (1999) 3772.
- [14] J. Chakravarty, S. Bhattacharya, Proc. Indian Acad. Sci. (Chem. Sci.) 107 (1995) 361 and refs. cited therein.
- [15] G.M. Sheldrick, SHELXL-Plus, Siemens, Analytical X-ray Instruments Inc., Madison, WI, 1990.
- [16] G.M. Sheldrick, Acta Crystallogr., Sect. A 46 (1990) 467.
- [17] G.M. Sheldrick, Program for refinement of crystal structures, University of Göttingen, Germany, 1997.
- [18] S. Chattopadhyay, N. Bag, P. Basu, G.K. Lahiri, A. Chakravorty, J. Chem. Soc., Dalton Trans. (1990) 3389.
- [19] D. Das, PhD Thesis, Burdwan University, Burdwan, India, 1998.
- [20] R.O. Gould, W.J. Sime, T.A. Stephenson, J. Chem. Soc., Dalton Trans. (1978) 76.
- [21] G.R. Clark, J.M. Waters, K.R. Whittle, J. Chem. Soc., Dalton Trans. (1975) 2556.
- [22] K. Nakamoto, Infrared Spectra of Inorganic and Coordination Compounds, 2nd edn., Wiley, New York, 1970, p. 175.
- [23] P. Majumdar, S. Goswami, S.-M. Peng, Polyhedron 18 (1999) 2543.
- [24] L.M. Jackman, Applications of Nuclear Magnetic Resonance Spectroscopy in Organic Chemistry, Pergamon Press, New York, 1959.
- [25] P. Chattopadhyay, C. Sinha, Polyhedron 13 (1994) 2689.
- [26] M. Menon, A. Pramanik, N. Bag, A. Chakravorty, J. Chem. Soc., Dalton Trans. (1995) 1543.
- [27] A. Pramanik, N. Bag, D. Ray, G.K. Lahiri, A. Chakravorty, J. Chem. Soc., Chem. Commun. (1991) 139.